

Fabrication of single-layer metallic nano-gratings as polarisers by the combination of nanoimprint lithography and lift-off method

Qianyi Wang, Jinkui Chu, Zhiwen Wang, Huixia Zhang, Ze Liu, Le Guan 

School of Mechanical Engineering, Dalian University of Technology, Dalian, Liaoning 116024, People's Republic of China

✉ E-mail: haishengtian@mail.dlut.edu.cn

Published in Micro & Nano Letters; Received on 18th August 2016; Revised on 30th October 2016; Accepted on 15th December 2016

To explore the application of miniaturised polarisers into the detection of the skylight polarisation angle, a fabrication process for single-layer metallic nano-gratings, which was treated as polarisers in the polarised light testing instrument, was proposed. With the help of the combination of two efficient fabrication methods, the nanoimprint lithography and the lift-off method, different directions of the metallic gratings with 200 nm period, 110 nm linewidth and 60 nm height were fabricated simultaneously on the substrate. An interval ultrasound method is proposed to avoid grating structure damage during the lift-off process. Additionally, the effect of the SiO₂ layer addition during the etching process on the transmission performance of metallic gratings is presented by a brief theory analysis and experiment results. The fabricated grating is installed on the designed testing instrument to measure the angle of polarised light and the final angle output error is within $\pm 0.25^\circ$, which demonstrates that the fabricated metallic gratings have a good prospect as a polaroid applied in the polarisation navigation.

1. Introduction: With the development of the nano-fabrication technology, some optical instruments become more and more miniaturised in size compared with the traditional ones. Based on the modern optical theory, the subwavelength metallic gratings have several unique properties on light transmission performance, which can be used as polarisers as well as light filter with appropriate designed structure [1–4]. In order to attain high performance of the transmission characteristic in visible spectrum and a wider testing angle [2], a kind of metallic gratings with hundreds nanometres period is proposed to fulfil the application in the polarised light detection [5–7]. Until today, several nano-scale fabrication methods have been introduced in metallic nano-gratings fabrication, such as electron beam lithography [7, 8], extreme interference lithography [9, 10] and nanoimprint lithography (NIL) [3, 11–16].

Comparing with other methods, the NIL is more and more commonly used in the nano-structure fabrication for its advantage of low cost, high resolution and efficient high-output for large area pattern. In the NIL process, the designed pattern can be easily replicated from the stamp to the imprint resist. Then the pattern transfers into the lower-layer resist by etching technology or other methods, in which the imprint resist is treated as a mask. Different fabrication processes are proposed for the single-layer metallic gratings combining with NIL, which can be summarised into several kinds of schemes: (i) etching the metal layer with a designed mask [3, 12]; (ii) removing the upper structure of a bilayer metallic grating to leave the bottom material to form the metallic grating [13–16] and so on. Although with a uniform metal layer for avoiding the uneven metal deposition on the rugged nano-structure, the direct etching metal process has its own difficulties in etching process such as expensive processing cost and need of appropriate etching mask and so on. Meanwhile, the lift-off process is widely used in the fabrication of metal patterns in micro-nano-scale. The various kinds of lift-off resist, lift-off solution and the adaption to several metal materials make it a more efficient and economical method comparing with the metal etching method.

In this Letter, we proposed a fabrication process of the single-layer metallic nano-gratings which are used as polarisers in the skylight polarisation angle detection instrument. Combining the NIL process and the lift-off method, multi-directional metallic gratings

are successfully fabricated on the glass substrate. An interval of ultrasound method is proposed to solve the difficulty of the lift-off process in nano-scale dimension. The influence of the SiO₂ layer addition in the etching process is discussed. The final performance of the fabricated metallic gratings is tested on the designed polarised light angle testing instrument to prove that the metallic gratings fabricated by proposed method can be applied in the skylight polarisation distribution detection as polarisers.

2. Fabrication process: The process flow designed for the single-layer metallic nano-gratings fabrication is shown in Fig. 1. The detailed description of the preparation process of metallic gratings is given: The lift-off resist PMGI (SF3, MICROCHEN) was spin coated on the substrate with a speed of 2000 rpm for 60 s and post-baked at 170°C for 4 min, followed by the SiO₂ deposition on the PMGI. The imprint resist (TU-7) was spin coated at 3000 rpm for 60 s on SiO₂ layer, with 95°C post-bake for 3 min. The thicknesses of three layers were 120, 45 and 120 nm, respectively. Subsequently, the designed pattern was transferred from the stamp to the imprint resist by NIL. The imprinting process was a critical step because NIL defined the resolution of the pattern on the imprint resist and the integrity of the pattern finally left on the substrate. The nickel stamp applied in this process with a dimension of 200 nm pitch and 80 nm linewidth was treated with anti-sticking monolayer of CF₃(CF₂)₇CH₂CH₂PO₂(OH)₂ (Hansa Fine Chemical, Germany) [17] to reduce the adhesion between the stamp and the resist during the demoulding process. The designed pattern was first transferred from the nickel stamp to a soft mould IPS® (Obducat AB, Sweden) by a hot imprinting process (40 bar, 160°C, 3 min). Then the pattern on the resist was defined by the imprinted IPS through a STU (simultaneous thermal and UV) imprinting process (40 bar, 95°C, 3 min), which applied hot imprinting and UV imprinting process simultaneously.

The inductively coupled plasma (ICP) etching process, carried out by AMS100SE (Alcatel, Ltd), was applied to remove the residual layer of imprint resist, and to etch the SiO₂ layer and the PMGI layer to expose the substrate. The parameters of three different ICP etching processes are shown in Table 1.

The thickness of deposition metal influences the performance of metallic gratings. However, during the actual fabrication process,

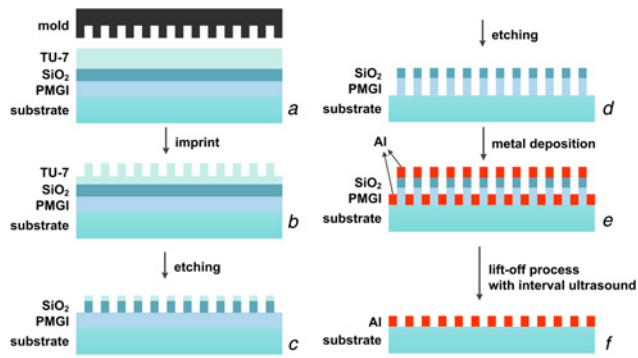


Fig. 1 Designed fabrication flow of the single-layer metallic nano-gratings

the thickness of the deposition metal is limited by two aspects: the thickness of PMGI and the self-shielding effect in the metal deposition process. Through a comprehensive consideration, 60 nm thickness Al was deposited on the structure to reach a better transmission characteristic. The PMGI with the upper structure was removed by the N-methyl kelopyrrolidide solution, leaving the bottom metal layer on the substrate. In order to improve the efficiency, an ultrasonic action is frequently used in the lift-off process [15, 16]. However, higher power and longer time ultrasound has a chance to destroy the structure of the nano-gratings. To solve this problem, the reduction of ultrasound power and the decomposition of the ultrasonic action were proposed. The process of interval ultrasound is presented in Table 2. The total time of the lift-off water bath process was about 30 min and every ultrasound time was controlled about 20 s to avoid structural damage caused by long time ultrasound. Actually, the specific lift-off time varied depending on the pre-baking condition of PMGI and the dimension of the gratings structure.

3. Discussion of the fabricated grating structure: After the interval ultrasound lift-off process, the single-layer metallic nano-gratings were successfully fabricated on the glass substrate, with six directions of 0, 30, 60, 90, 120 and 150° (Fig. 2). The cross-sectional scanning electron microscope (SEM) image of the fabricated metallic gratings is shown in Fig. 2a, with the structure of 60 nm height, 200 nm period and 110 nm linewidth. Fig. 2b presents the surface morphology of the metallic gratings with a good linearity.

As previously discussed, the SiO₂ layer acts as the etching mask of the PMGI resist. Without the SiO₂ layer addition, due to the fact

Table 1 Parameters of three different ICP etching processes

Etching layer	Gas	Pressure, mbar	Gas flow, sccm	ICP power, W	RF power, W	Time, s
TU-7	O ₂	7.6×10^{-3}	200	40	200	20
SiO ₂	C ₄ F ₈	7.6×10^{-3}	50	300	2800	25
PMGI	O ₂	7.6×10^{-3}	200	160	160	65

Table 2 Outline of interval ultrasound method

Method	Parameters	Time
water bath	70°C	5–8 min
ultrasound	40% of rated power	10–20 s
water bath	70°C	5–8 min
ultrasound	40% of rated power	10–20 s
water bath	70°C	14–20 min

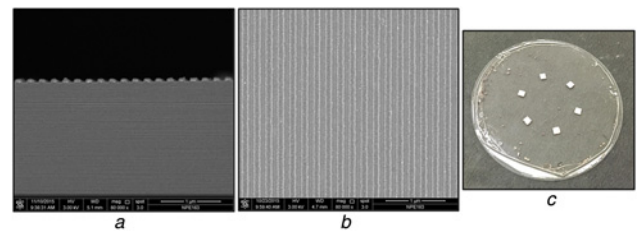


Fig. 2 SEM images and integral image for the fabricated metallic nano-gratings

a Cross-section SEM image

b Top-view SEM image

c Integral image of six directions metallic gratings

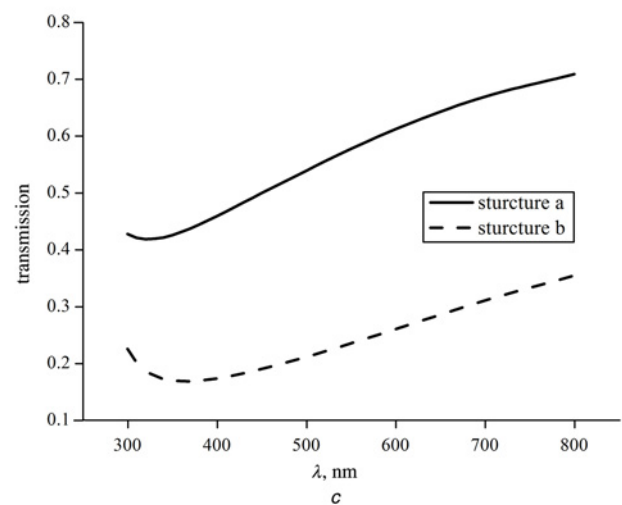
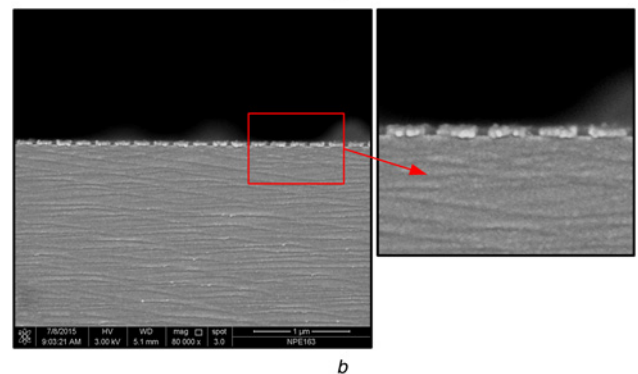
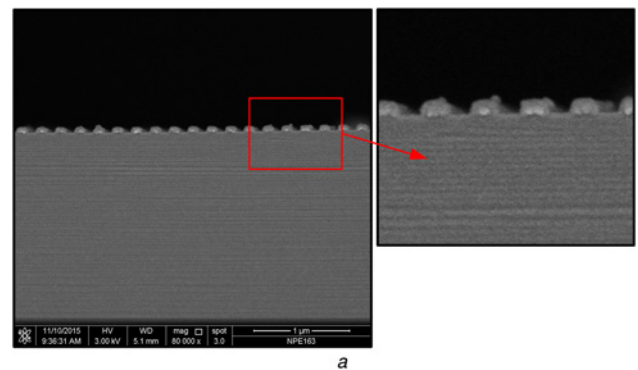


Fig. 3 Cross-sectional SEM images of metallic gratings structures with different fabrication process and the theoretical analysis of these two structures

a Introduced the SiO₂ layer

b Without the SiO₂ layer

c Theory analysis of TM transmission

that TU-7 and PMGI share the same etching gas O_2 , the duty cycle of the gratings increased with the window of TU-7 mask expanded during the PMGI etching process, which, in the end, result in the decrease of metallic grating transmission. In order to analyse how the SiO_2 layer affects the final grating structure, we also developed a process without the SiO_2 layer. Except the SiO_2 layer deposition and etching process, the other processes are the same as shown in Fig. 1, including the stamp dimension and the special lift-off process with interval ultrasound. The cross-sectional SEM images of metallic gratings fabricated by the 'double-layer' process is shown in Fig. 3b, with a duty cycle larger than 0.7. Furthermore, the discussion on the transmission characteristic of the metallic gratings influences by the SiO_2 layer addition is under the analysis by the rigorous coupled-wave analysis [18]. As shown in Fig. 3, even the structure models resulting from triple-layer process and double-layer process share the same metallic gratings period of 200 nm, the linewidths of the two gratings are 110 nm (Fig. 3a) and 150 nm (Fig. 3b), respectively. According to the theoretical analysis, the transverse magnetic (TM) transmission of the structure a (solid line in Fig. 3c, 110 nm linewidth) is about two times as much as the structure b (dashed line in Fig. 3c, 150 nm linewidth) under the grating height of 60 nm. The result demonstrates the importance of the SiO_2 layer in the designed structure as the mask of the PMGI resist to reduce the duty cycle.

4. Polarisation angle test: According to the bionics theory [5, 6], that the polarisation pattern in the sky can be utilised to navigation field, metallic nano-gratings with multi-directions are fabricated on one substrate to determine the angle of the polarised light. As shown in Fig. 2, six metallic gratings with the direction of 0, 30, 60, 90, 120 and 150° are successfully fabricated on the glass substrate during the same process, getting rid of fix-errors. Fig. 4 illustrates the polarisation angel test instrument, which comprised of an integrating sphere, a polariser sheet, a testing sample, photoelectric detectors, a polarisation navigation sensor, a rotary platform and a computer for data collection and processing as discussed in previous papers [5, 6]. The testing light with uniform intensity distribution, provided by the integrating sphere,

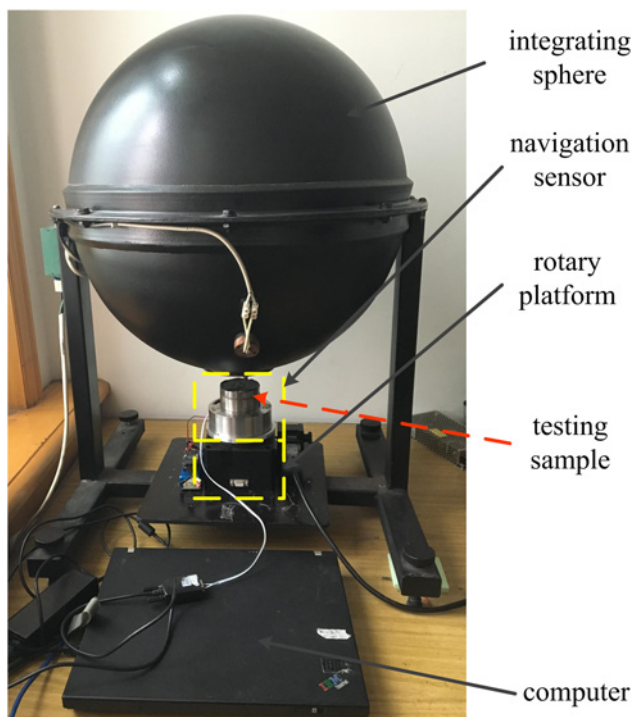


Fig. 4 Illustration of the polarised light angle test instrument

turns to polarisation through the polarisers, and then strikes to the metallic gratings. Based on the photoelectric detector and the navigation sensor, the light signal from the metallic gratings is collected and transferred to an amplified voltage signal.

To calculate the angle of the polarised light, the six directions gratings along with the corresponding photoelectric detector are separated into three units: 0°/90°, 30°/120° and 60°/150°. Every signal in the single detect unit is amplified by a log-ratio amplifier (Log100, Texas Instrument Inc., USA) in order to calculate the difference of the two logarithmised signals in a unit. According to (1)–(4) [5], the voltage values of three units can be described by polarisation angle θ and polarisation degree d_p . Based on the inverse logarithm transform and the trigonometric function operation, the d_p and θ can be resolved, thus the final direction of the test instrument reference to the solar meridian can be deduced and shown in (4):

$$V_1(\theta) = 0.5 \log \left(\frac{1 + d_p \cos(2\theta)}{1 - d_p \cos(2\theta)} \right) \quad (1)$$

$$V_2(\theta) = 0.5 \log \left(\frac{1 + d_p \cos(2\theta - (2\pi/3))}{1 - d_p \cos(2\theta - (2\pi/3))} \right) \quad (2)$$

$$V_3(\theta) = 0.5 \log \left(\frac{1 + d_p \cos(2\theta - (4\pi/3))}{1 - d_p \cos(2\theta - (4\pi/3))} \right) \quad (3)$$

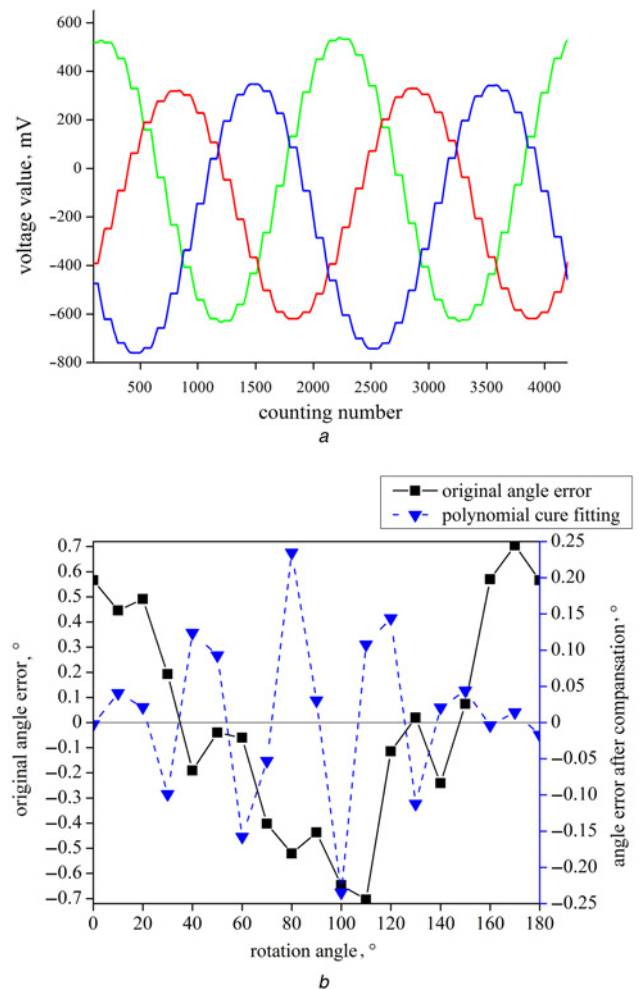


Fig. 5 Angle test results of testing sample with six directions metallic nano-gratings
a Voltage output of the three units with the platform rotating
b Angle errors of the testing results

$$\theta = \frac{1}{2} \tan^{-1} \left\{ \frac{P_1(\theta) + 2P_2(\theta) - (3/2)}{\sqrt{3}[P_1(\theta) - (1/2)]} \right\} \quad (4)$$

where $P_i(\theta) = 1/(10^{V_i} + 1)$ ($i = 1, 2, 3$) refers to the logarithmic transformation of $V_i(\theta)$.

Fig. 5a illustrates the output voltage signals of the three units with the rotation angle increasing every 10° , in which the peak positions are evenly 60° apart. The central positions of the three curves deviation from the x -axis and the non-uniform amplitudes output can be normalised before calculating the angle output error. The result of the angle error is about $\pm 0.7^\circ$ without any compensation as shown in Fig. 5b by the solid line. Therefore, a polynomial cure fitting with an order of 11 is applied for the angle error compensation, thus the angle error is optimised within $\pm 0.25^\circ$ (Fig. 5b, the dash line).

By analysing the factors that influence the angle error shown in Fig. 5b, there are two main reasons as we discussed leading to the error, the defects caused by the gratings fabrication process and the effects caused by the testing process. The influence of the pattern non-uniformity can be transferred and expanded through the pattern replication process, which leads to the different polarisation performance of every direction of metallic gratings in the testing sample. The etching process and the lift-off process also have the possibility to impact the surface homogeneity of the metallic gratings. What is more, the alignment of the testing sample to the photoelectric detector and the inconsistency of the six photoelectric detectors also have the influence on the result of the angle error. Therefore, an integration device aiming to fabricate the metallic grating on the photoelectric detector is a promising method to reduce the testing error.

5. Conclusion: In this Letter, we designed a process that combined two economical and effective methods to fabricate single-layer metallic nano-gratings with 200 nm period and 110 nm linewidth. The comparison of the grating transmission performance proves that the importance of the addition of the SiO_2 layer, and that the proposed interval ultrasound method ensures the integrity of the pattern and the good polarisation performance of the metallic gratings. This kind of fabrication process also can be applied in the fabrication of a metal mask with nano-scale. The final angle output error along with these metallic gratings on the test instrument is within $\pm 0.25^\circ$ under the error compensation. For a further study, the proposed metal-gratings fabrication method can be integrated with the photoelectric detector to achieve a better performance in the detection of the direction of the polarisation light.

6. Acknowledgments: This work was supported by the National Basic Research Program of China (grant nos. 2011CB302101 and 2011CB302105) and, the National Natural Science Foundation of China (grant nos. 51305057, 51675076, 51505062) and the Science Fund for Creative Research Groups of NSFC (grant no. 51621064).

7 References

- [1] Schider G., Krenn J.R., Gotschy W., *ET AL.*: 'Optical properties of Ag and Au nanowire gratings', *J. Appl. Phys.*, 2001, **90**, (8), pp. 3825–3830
- [2] Yu X.J., Kwok H.S.: 'Optical wire-grid polarizers at oblique angles of incidence', *J. Appl. Phys.*, 2003, **93**, (8), pp. 4407–4412
- [3] Wang J.J., Chen L., Liu X., *ET AL.*: '30-nm-wide aluminum nanowire grid for ultrahigh contrast and transmittance polarizers made by UV-nanoimprint lithography', *Appl. Phys. Lett.*, 2006, **89**, (14), p. 141105
- [4] Meng F., Luo G., Maximov I., *ET AL.*: 'Fabrication and characterization of bilayer metal wire-grid polarizer using nanoimprint lithography on flexible plastic substrate', *Microelectron. Eng.*, 2011, **88**, (10), pp. 3108–3112
- [5] Chu J.K., Wang Z.W., Guan L., *ET AL.*: 'Integrated polarization dependent photodetector and its application for polarization navigation', *IEEE Photonics Technol. Lett.*, 2014, **26**, (5), pp. 469–472
- [6] Chu J.K., Zhao K.C., Zhang Q., *ET AL.*: 'Construction and performance test of a novel polarization sensor for navigation', *Sens. Actuators A, Phys.*, 2008, **148**, (1), pp. 75–82
- [7] Gao S., Njuguna R., Gruev V.: 'Fabrication and performance evaluation of pixelated nano-wire grid polarizer'. Polarization Science and Remote Sensing VI, 2013, vol. 8873, pp. 88730L
- [8] Schnabel B., Kley E.B.: 'Fabrication and application of subwavelength gratings'. Miniaturized Systems with Micro-Optics And Micromechanics II, 1997, vol. 3008, pp. 233–241
- [9] Auzelyte V., Dais C., Farquet P., *ET AL.*: 'Extreme ultraviolet interference lithography at the Paul Scherrer Institut', *J. Micro-Nanolith. Mem.*, 2009, **8**, (2), pp. 75–78
- [10] Brueck S.R.J.: 'Optical and interferometric lithography – nanotechnology enablers', *Proc. IEEE*, 2005, **93**, (10), pp. 1704–1721
- [11] Chou S.Y., Krauss P.R., Renstrom P.J.: 'Imprint of sub-25 nm vias and trenches in polymers', *Appl. Phys. Lett.*, 1995, **67**, (21), pp. 3114–3116
- [12] Ahn S.W., Lee K.D., Kim J.S., *ET AL.*: 'Fabrication of subwavelength aluminum wire grating using nanoimprint lithography and reactive ion etching', *Microelectron. Eng.*, 2005, **78–79**, pp. 314–318
- [13] Wu W., Kim E., Ponizovskaya E., *ET AL.*: 'Optical metamaterials at near and mid-IR range fabricated by nanoimprint lithography', *Appl. Phys. A, Mater.*, 2007, **87**, (2), pp. 143–150
- [14] Zhang R., Chu J.K., Wang Z.W., *ET AL.*: 'Simple process for single-layer nanowire gratings', *Micro Nano Lett.*, 2015, **10**, (5), pp. 272–275
- [15] Wu C.L., Yao P.H., Lin C.H., *ET AL.*: 'Fabrication of flexible metallic wire grid polarizer using thermal NIL and lift-off processes', *Microelectron. Eng.*, 2012, **98**, pp. 117–120
- [16] Calafiore G., Dhuey S., Sassolini S., *ET AL.*: 'Multilayer lift-off process for sub-15-nm patterning by step-and-repeat ultraviolet nanoimprint lithography', *J. Micro-Nanolith. Mem.*, 2014, **13**, (3), pp. 1654–1658
- [17] Keil M., Beck M., Ling T.G.I., *ET AL.*: 'Development and characterization of silane antisticking layers on nickel-based stamps designed for nanoimprint lithography', *J. Vac. Sci. Technol. B*, 2005, **23**, (2), pp. 575–584
- [18] Moharam M.G., Gaylord T.K.: 'Rigorous coupled-wave analysis of planar-grating diffraction', *J. Opt. Soc. Am.*, 1981, **71**, (7), pp. 811–818